Int. J. Electrochem. Sci., 15 **(2020)** 2430 – 2438, doi: 10.20964/2020.03.56

International Journal of ELECTROCHEMICAL SCIENCE
www.electrochemsci.org

Short Communication

High Strain Sensitivity of Concrete incorporated with Silica Nanoparticles and Corrosion of reinforced steel in NaCl solution

Changyin Gan

College of Materials and Chemical Engineering, Hainan University, Haikou, Hainan, 570228, China
E-mail: ganchangyin@163.com

Received: 17 October 2019/ *Accepted:* 23 December 2019 / *Published:* 10 February 2020

In this research, the concentration effect of silica nanoparticles on electrochemical and strain sensitivity of smart polymer concretes were investigated. Silica nanoparticles with uniform and spherical morphology was synthesized by in situ sol-gel method. The structural properties of synthesized silica nanoparticles were studied by X-ray diffraction and Fourier transform infrared analyses, showing the amorphous and high stable phase of the nanoparticles. Strain sensitivity of smart polymer concrete was enhanced with increasing the concentration of silica nanoparticles in concretes. A very large variation of resistance was observed under mechanical strain because of higher mobility of silica nanoparticles and their stronger adhesion to the polymer matrix. Electrochemical corrosion of steel rebars were considered by electrochemical impedance spectroscopy technique which indicated that the addition of silica nanoparticles in cement content led to improve the thickness, corrosion resistance and stability of passive film on steel rebar.

Keywords: Smart polymer concrete; Silica nanoparticles; Strain sensitivity; Electrochemical impedance spectroscopy

1. INTRODUCTION

Concrete is the main material in the construction industries due to its essential strength properties. However, the concrete properties can be improved by adding some other materials. With the increasing approach to the use of concrete in high-rise buildings, there is a great demand for higher compressive strength concrete [1-3]. Nanotechnology is one of the ways to improve the properties of materials that lead to optimization of their application in various industries [4]. The use of nanotechnology in the building materials especially in concretes has received more attention because of its improved sustainability, durability and mechanical properties [5, 6]. This evolution in concrete composition lead to new generation of concretes that are well-known to smart concretes.

Smart concrete can be useful for improving traffic efficiency, increasing the lifespan of structures, reducing the source and energy consumption [7].

Recently, the use of nanostructures to develop the concrete properties has formed a new perspective on smart concrete technology [8, 9]. Researches show an enhancement in concrete properties especially higher strength by addition of silica particles in nano and micro scale to concrete mixes [10-12]. Therefore, silica nanocomposite is selected to study on smart concrete due to the similarity of its chemical composition with silicate layers and its particle shape.

In this study, the silica nanoparticles were synthesized in situ sol-gel method. The structural properties of synthesized silica nanoparticles were studied by The XRD and FTIR analyses. Then, smart polymer concretes with mixed polypropylene fibers and different concentrations of silica nanoparticles (0, 0.5, 1, 2 wt%) were prepared. Finally, the strain sensitivity and electrochemical corrosion of steel rebar in smart polymer concrete were studied.

2. MATERIALS AND METHOD

In order to synthesize silica nanoparticles, cation exchange membranes (Nafion 115, Dupont, USA) was cleaned out in a 4 wt% H_2O_2 solution at 65–85 ºC for 25 minutes. Then, the membranes were immersed in 1 mol dm^{-3} H_2SO_4 solution for 25 minutes and rinsed with DI water to eliminate any remaining drop of H_2O_2 and H_2SO_4. A conventional in situ sol-gel method was used to synthesize the silica nanoparticles using tetraethyl orthosilicate ($Si(OCH_2CH_3)_4$) as a precursor for reaction with water-methanol solvent. The membranes were soaked in a 25 mL Methanol/tetraethyl orthosilicate solution in the ratio of 1:1 for 12 hours. The methanol facilitates the permeation of water and tetraethyl orthosilicate solution into the membrane channel. The membranes were then immersed in a 40 mLsolution with methanol and ammonia in the ratio of 1:1 under intense stirring to start the reaction of hydrolysis/condensation to form the silica nanoparticles. Furthermore, ammonia as a catalyst was used to provide an alkaline medium. Finally, the obtained silica nanoparticles were immediately immersed in anhydrous methanol to eliminate the surplus reactants and dried under ambient condition for 12 hours.

The smart polymer concretes were prepared by combination of polypropylene fibers and different concentrations of silica nanoparticles. The materials used for the concrete mixture were Water, Cement, Aggregate in 250 kg m^{-3}, 400 kg m^{-3} and 1760 kg m^{-3}, respectively. The concrete mixture was put in frames with 25 mm diameters and height of 190 mm. 2 kg m^{-3} polypropylene fibers were added in concrete mixture in the rotating mixer. Then, different concentrations of silica nanoparticles (0, 0.5, 1 and 2 wt%) were added.

An electronic universal testing machine was used to investigate axial compression on blocks with loading rate of 0.5 mm/min. The block resistance was determined by using two steel mesh electrode technique, and the resistance values were gathered by a digital multimeter.

A 1.5 wt% NaCl electrolyte solution was utilized in electrochemical impedance spectroscopy (EIS) analysis. The pH of solution was adjusted by $NaHCO_3$ at 12.0. pH meter (Sigma, P1367 MSDS) was applied for adjusting the pH of solutions. The ordinary concrete was prepared the same condition of the smart polymer concrete, but it was not containing any silica nanoparticles. In order to study the

corrosion properties of steel rebar, a low carbon steel rebar with 6 mm diameter was used. The steel rebars were polished by 2400-grade silicon-carbide papers (LANHU, Germany) and cleaned in acetone solution and DI water. The conventional three-electrode electrodeposition cell was conducted for electrochemical analysis that it contains steel rebar, a platinum wire and a saturated calomel as working electrode, counter electrode and reference electrode, respectively. Before the electrochemical analysis the samples were immersed in electrolyte solution for 4 weeks. EIS (CorrTest Instruments Corp., Ltd., China) tests were performed at a scanning range of 10 mHz to 100 kHz at the amplitude of 10 mV.ZSimpWin was used to interpret the experimental results.

The crystalline phases of the samples were characterized by a D8 Advance (Bruker) X-ray diffractometer (XRD) with Cu Kα radiation (λ = 0.154 nm). Fourier transform infrared spectra (FTIR) was obtained employing the FTIR spectrometer (Thermo electron corporation, Nexus 670, USA) in the wavenumber region of 400 to 4000 cm^{-1}.The morphologies of the samples were examined using scanning electron microscope (SEM, Hitachi-3000).

3. RESULTS AND DISCUSSION

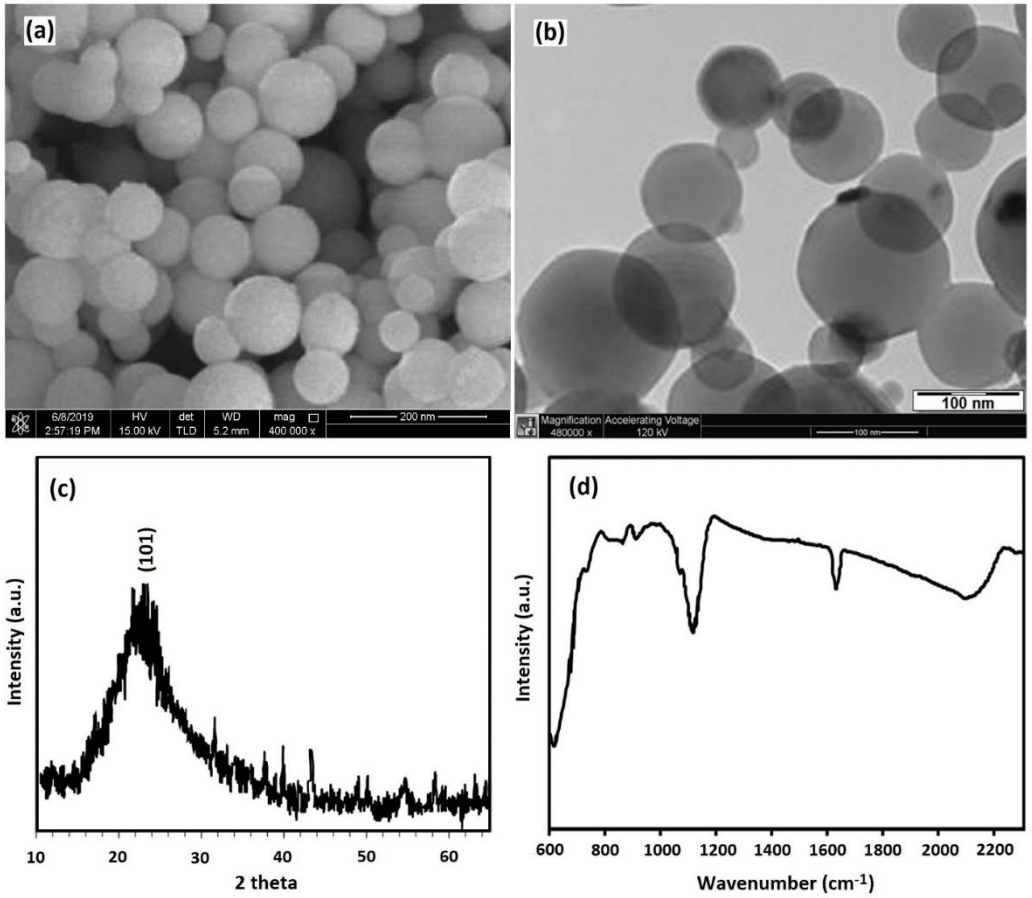

Figure 1. (a) FESEM, (b) TEM images, (c) XRD patterns and (d) FTIR spectra of synthesized silica nanoparticles.

The spherical morphology and uniformity of the as-prepared silica nanoparticles are clearly seen in FESEM image indicated in figure 1a. The TEM image of silica nanoparticles were presented in figure 1b which clearly shows the size of synthesized nanoparticles are between 70 to 150 nm. Production of

silica nanoparticles can be confirmed by XRD analysis. The X-ray diffraction patterns of the synthesized silica nanoparticles are shown in Figure 1c. A broad peak of (101) appeared in the range of 16°–38° which indicates the amorphous nature of silica nanoparticles.

The FTIR spectra of the synthesized silica nanoparticles is shown in Figure 1d. It clearly showssome spectral peaks at 950 cm^{-1} and 1090 cm^{-1} according to asymmetric vibration (Si–OH and Si–O) and a peak at 793 cm^{-1} from symmetric vibration (Si–O) [13]. The absorption bands between 800 and 1260 cm^{-1} have been described as a superimposition of various SiO_2 peaks due to residual organic groups [14]. Moreover this band can be cross checked through the 1640 cm^{-1} band due to scissor bending vibration of molecular water.

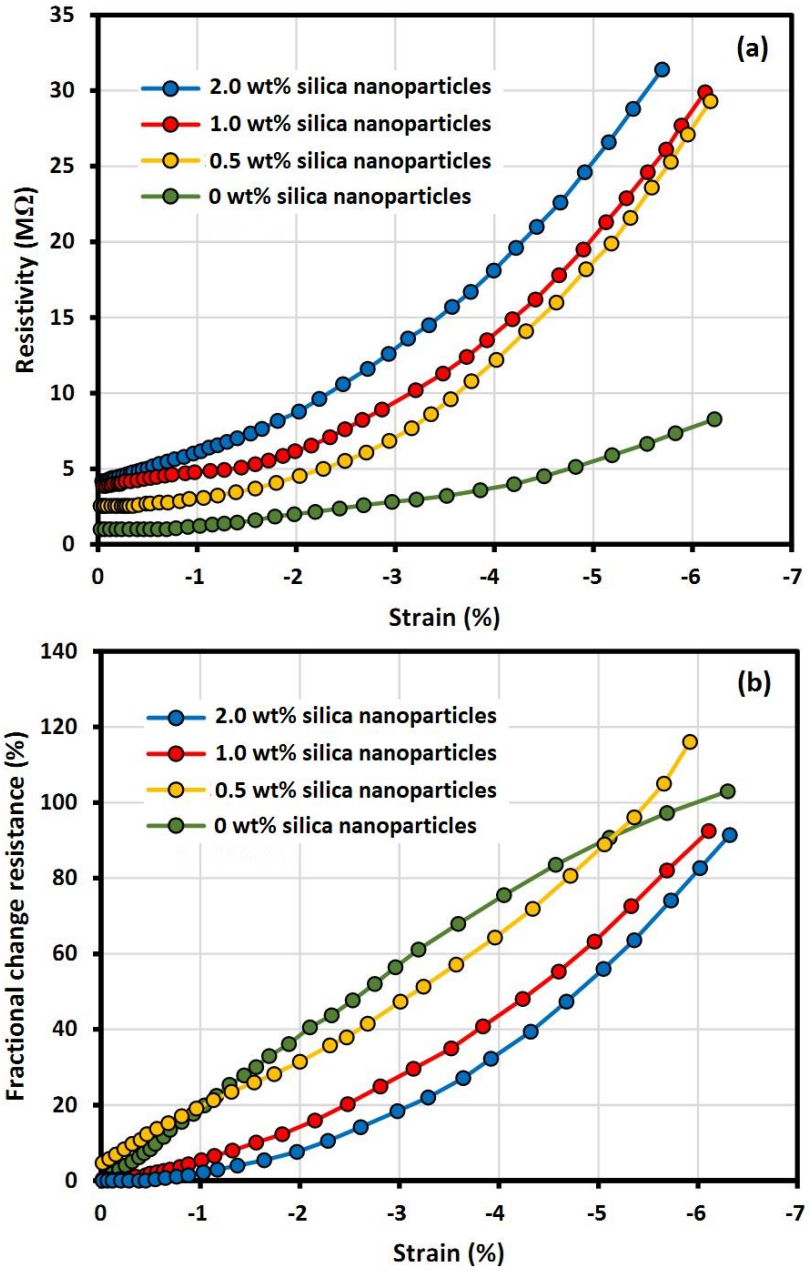

Figure 2. (a)Resistance versus strain and (b) fractional change in resistance versus strain for the smart polymer concretes prepared with different concentrations of silica nanoparticles.

In order to evaluate the strain sensitivity of the samples, the resistivity–strain dependence was investigated. Despite the different starting points because of the various filler concentrations, the general trend indicated that the resistivity in all samples increases by strain increasing. As shown in figure 2a, a small change in silica nanoparticle content leadsto a significantly change in the slope of the resistivity–strain plot, indicating a wide-range of sensitivities. It was clarified by the contact loss between silica nanoparticles in the matrix and developed tunneling resistance. The strain sensitivity curve of samples without silica nanoparticles is relatively discrete. The initial analysis for this phenomena can be attributed to the different conductivity of smart polymer concretes, which can be reflected in the different concentrations of silica nanoparticles and different initial resistance of experiment for each sample. This result agrees with previous studies which found that composites at the electrical threshold commonly reveal the largest change in electrical resistance by applied strain because of larger changes in the conductive networks [15, 16]. According to the above findings, an appropriate concentrations of Nano-silica fillers can be chosen to enhance a desired strain sensitivity in sensing applications of large deformation.

The fractional change in resistance to the strain for the concrete blocks with different silica nanoparticle content are shown in Figure 2b. In order to analyzethe sample behavior, a quadratic function was applied to fit the data scatter diagram of resistance-strain and fractional change in resistance that these functions correspond to $y = Ax^2 + B$. Where A and B are constants that refer to the material of smart polymer concretes. The x and y are two variables associated with the strain (%) and the resistance (MΩ), respectively. In order to determine the degree of relationship between two variables x and y, the correlation coefficient (R^2) was calculated. Table 1 showsthe obtained parameters of fitting process**.** Hence, the coefficient Acan be applied to determine the strain sensitivity of smart polymer concrete.

Table 1. The obtained parameters of fitting the resistance-strain curves of smart polymer concrete samples prepared with different concentrations of silica nanoparticles

Concentrations of silica nanoparticles	R^2	A	B
0.0 wt%	0.9981	6.01	1.59
0.5 wt%	0.9979	8.99	3.08
1.0 wt%	0.9987	17.58	8.64
2.0 wt%	0.9988	36.15	15.02

The results show that the strain sensitive curves are in good accordance with the quadratic curves and the resistance of the samples increases gradually with the strain in the early stages, and then increases quickly with the increase of the strain.

Given that the silica nanoparticles exhibit pozzolanic and cementitious properties, thus, addition of silica nanoparticles can affect mechanical concrete behavior. When water is added to cement, hydration occurs which lead to the formation of two products calcium silicate hydrate and $Ca(OH)_2$. After addition of silica nanoparticles to the cement composition, the silicon dioxide from the silica nanoparticles react with the calcium hydroxide to produce more aggregate binding calcium silicate hydrate [17]. The reaction decreasesthe amount of $Ca(OH)_2$ in the concrete which does not help to strengthen the concrete. When $Ca(OH)_2$ combines with carbon dioxide, a soluble salt forms which is a

well-known architectural problem. Once high amounts of $Ca(OH)_2$ are present in concrete, the concrete is more vulnerable to adverse alkali-aggregate reactions, chemical attack and sulfate attack. Therefore, chemical composition silica nanostructures show a considerable change in the concrete structure. The nano-sized structure of the silica nanoparticles can fill all of pores in concrete and can provide conductive interface layer in smart polymer concrete. Therefore, the addition of the silica nanoparticles helps to promote the conductivity of adhesive system.

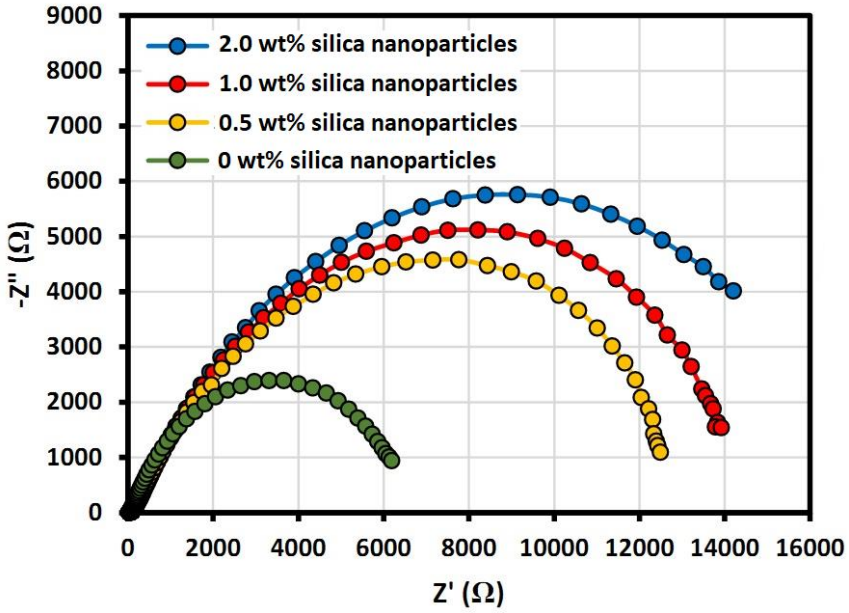

Figure 3. Nyquist plots obtained from steel rebars at 1.5 wt% NaClsolution for the smart polymer concretes prepared with different concentrations of silica nanoparticles.

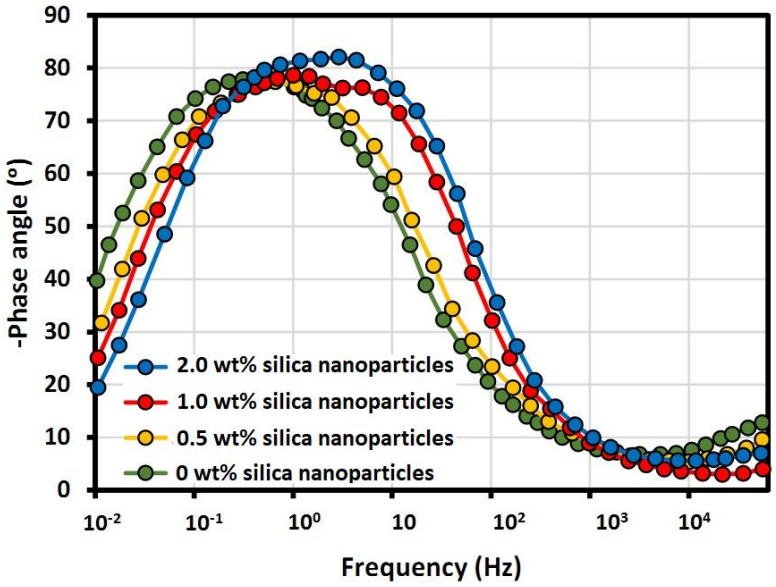

Figure 4. Bode phase plot of the steel rebars at 1.5 wt% NaCl solution for the smart polymer concretes prepared with different concentrations of silica nanoparticles.

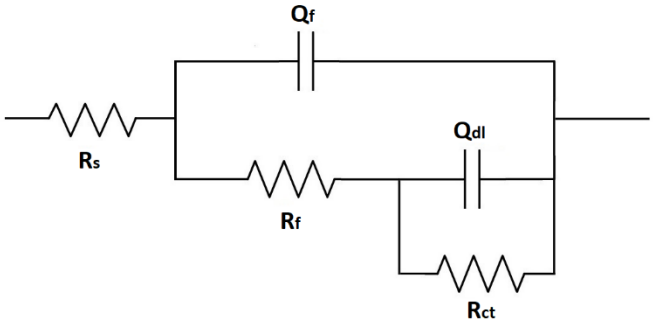

Figure 5. An equivalent electrical circuit model

Table 2. The obtained parameters of fitting the Nyquist plots for steel rebars in smart polymer concrete samples prepared with different concentrations of silica nanoparticles

Content of silica nanoparticles	R_s (Ω)	R_f (kΩ)	Q_f(μF cm^{-2})	R_{ct} (kΩ)	Q_{dl}(μF cm^{-2})
0.0 wt%	8.5	4.22	6.2	6.75	8.5
0.5 wt%	6.8	7.53	4.3	12.94	6.9
1.0 wt%	7.4	9.85	3.1	14.63	4.7
2.0 wt%	7.7	11.28	1.9	18.86	2.6

EIS technique has been used for studies of the corrosion behavior of steel rebars in smart polymer concrete prepared by different concentrations of silica nanoparticles. The Nyquist plots obtained from the EIS analysis was shown in Figure 3. As shown in figure 4, the phase angle was quickly increased at low frequencies with the addition of silica nanoparticles. The highest value was obtained at approximately 1 Hz excitation frequency, indicating the passive layer of steel can be locally damaged and pitting corrosion may hadoccurred [18]. With the addition of 2 wt% silica nanoparticles in the concrete, the phase angle was constantly shifted to approximately 10 Hz excitation frequency, indicating the chargeof thetransfer rate was enhanced and the mass transfer mightbecome themain parameter governing the rate of corrosion. The used of equivalent circuit model is shown in Figure 6. Wherein R_s is the solution resistance.Q_f andR_f represent the constant phase element (CPE) and the resistance element for corrosion products layer formed on the steel rebar, respectively [19]. Q_{dl} andR_{ct} are the CPE of the double-layer capacitance and the charge transfer resistance, respectively [20]. The calculated dataare presented in Table 2.

As shown in table 2, with the addition of silica nanoparticles inthecement content, $Q_f$decreases and R_f increases, which indicates that the increase of silica nanoparticles enhances the thickness, corrosion resistance and stability ofthepassive film on the steel rebar. The silica nanoparticles gave a pozzolanic reaction to the $Ca(OH)_2$ crystals and formeda dense, monolithic and insoluble gel of calcium hydroxide [21]. Due to the high surface area of silica nanoparticles, it can form a very strong adhesion to the hydrated cement and leadsto a betterprevention of the growth of calcium hydroxide crystals. The nanoparticles fill the tiny cracks and capillary pores and eventually condense the cement structure. These factors enhance the corrosion resistance of steel rebar in aggressive solutions.

4. CONCLUSION

The nanomaterials incorporated in the building materials especially in concretes has received more attention because of its improved sustainability, durability and mechanical properties. Here, the smart polymer concretes with different concentration of silica nanoparticles were prepared and their strain sensitivity and electrochemical properties were studied. The in situ sol-gel technique was used in thepreparation of silica nanoparticles. FESEM and TEM images of the as-prepared silica nanoparticles were clearly indicated the uniform and spherical morphology. The structural characterization of silica nanoparticles showed an amorphous structure and high phase stability. The strain-sensitive properties of smart polymer concretes were in good accordance with the quadratic curve. When silica nanoparticles concentration was increased in the concrete composition, the strain sensitivity of the samples increased. The EIS results revealed that the addition of silica nanoparticles in cement content had led to an enhancement in the thickness, corrosion resistance and stability of passive film on steel rebar. The silica nanoparticles filled the tiny cracks and capillary pores and eventually condensedthe cement structure. These factors led towards promotingthe corrosion resistance of steel rebar in corrosive solution and enhance the strain sensitivity of concrete.

ACKNOWLEDGEMENTS
The study was supported by “Science and Technology Project of China Railway Corporation, China (Grant No. 1341324011)”.

References

1. U. Sharma, A. Khatri and A. Kanoungo, *International Journal of Civil Engineering Research*, 5(2014)9.
2. M.M. Johari, J. Brooks, S. Kabir and P. Rivard, *Construction and Building Materials*, 25(2011)2639.
3. P. Shao, L. Ding, J. Luo, Y. Luo, D. You, Q. Zhang and X. Luo, *ACS applied materials & interfaces*, 11(2019)29736.
4. M.M. Norhasri, M. Hamidah and A.M. Fadzil, *Construction and Building Materials*, 133(2017)91.
5. J. Wang, Y.C. Ersan, N. Boon and N. De Belie, *Applied microbiology and biotechnology*, 100(2016)2993.
6. P. Shao, X. Duan, J. Xu, J. Tian, W. Shi, S. Gao, M. Xu, F. Cui and S. Wang, *Journal of hazardous materials*, 322(2017)532.
7. C.K. Leung, J. Yu, D.K. Mishra and A.K. Das, *Advances in Civil Engineering Materials*, 8(2019)1.
8. V. Volpi-León, L. López-Léon, J. Hernández-Ávila, M. Baltazar-Zamora, F. Olguín-Coca and A. López-León, *International Journal of Electrochemical Science*, 12(2017)22.
9. L. Yang, G. Yi, Y. Hou, H. Cheng, X. Luo, S.G. Pavlostathis, S. Luo and A. Wang, *Biosensors and Bioelectronics*, 141(2019)111444.
10. G. Perez, E. Erkizia, J. Gaitero, I. Kaltzakorta, I. Jiménez and A. Guerrero, *Materials Chemistry and Physics*, 165(2015)39.
11. C. Li, S. Hu, L. Yang, J. Fan, Z. Yao, Y. Zhang, G. Shao and J. Hu, *Chemistry–An Asian Journal*, 10(2015)2733.

12. G. Cao, L. Wang, Z. Fu, J. Hu, S. Guan, C. Zhang, L. Wang and S. Zhu, *Applied Surface Science*, 308(2014)38.
13. D. Sun, S. Kang, C. Liu, Q. Lu, L. Cui and B. Hu, *International Journal of Electrochemical Science*, 11(2016)8520.
14. J. Hu, C. Zhang, B. Cui, K. Bai, S. Guan, L. Wang and S. Zhu, *Applied Surface Science*, 257(2011)8772.
15. G. Georgousis, C. Pandis, A. Kalamiotis, P. Georgiopoulos, A. Kyritsis, E. Kontou, P. Pissis, M. Micusik, K. Czanikova and J. Kulicek, *Composites Part B: Engineering*, 68(2015)162.
16. S. Wang, X. Zhang, X. Wu and C. Lu, *Soft Matter*, 12(2016)845.
17. A. Sierra-Fernandez, L.S. Gomez-Villalba, M.E. Rabanal and R. Fort, *Materiales de Construcción*, 67(2017)107.
18. H.-S. Lee, H.-M. Yang, J.K. Singh, S.K. Prasad and B. Yoo, *Construction and Building Materials*, 173(2018)443.
19. K.M. Emran and H. AL-Refai, *International Journal of Electrochemical Science*, 12(2017)6404.
20. N. Naderi, M. Hashim, K. Saron and J. Rouhi, *Semiconductor Science and Technology*, 28(2013)025011.
21. J. Setina, A. Gabrene and I. Juhnevica, *Procedia Engineering*, 57(2013)1005.